Renewable and Sustainable Energy Reviews 32 (2014) 548–558

Contents lists available at ScienceDirect

Renewable and Sustainable Energy Reviews

journal homepage: www.elsevier.com/locate/rser

A review of direct torque control of induction motors for sustainable reliability and energy efficient drives

Tole Sutikno [a,b], Nik Rumzi Nik Idris [b,c,d,*], Auzani Jidin [e]

[a] Department of Electrical Engineering, Faculty of Industrial Technology, Universitas Ahmad Dahlan 3rd Campus, Jln. Prof. Soepomo, Janturan, Yogyakarta 55164, Indonesia
[b] Department of Energy Conversion, Faculty of Electrical Engineering, Universiti Teknologi Malaysia, 81310 UTM Skudai, Johor, Malaysia
[c] Power Electronics and Drives Research Group (PEDG), Universiti Teknologi Malaysia, 81310 UTM Skudai, Johor, Malaysia
[d] UTM-PROTON Future Drive Laboratory, Universiti Teknologi Malaysia, 81310 UTM Skudai, Johor, Malaysia
[e] Department of Power Electronics & Drives, Faculty of Electrical Engineering, Universiti Teknikal Malaysia Melaka, Hang Tuah Jaya, 76100 Durian Tunggal, Melaka, Malaysia

ARTICLE INFO

Article history:
Received 30 July 2013
Received in revised form
19 December 2013
Accepted 4 January 2014
Available online 5 February 2014

Keywords:
Direct torque control
Electric vehicle
Energy efficient
Future transportation
Induction motor

ABSTRACT

The first and the most important step in solving the environmental problems created by cars with internal combustion engines is research and development of electric vehicles. Selection of a proper drive and optimal control strategy of electric vehicles are the major factors to obtain optimal energy management in order to extend the running distance per battery charge. This paper presents a brief review of direct torque control (DTC) of induction motors (IM) as well as its implementation for electric vehicle (EV) applications. First, the basic DTC technique based on hysteresis controllers will be introduced, and then an overview of the major problems in a basic DTC scheme will be presented and explained, as well as some efforts for improving the technique. The main section presents a critical review of DTC for EV applications, taking into consideration the vehicle mechanics and aerodynamics of electric vehicles. The review is very important to provide guidelines and insights for future research and development on the DTC of IM drives for sustainable reliability and energy efficient EV applications.

Contents

1. Introduction . . . 549
2. Direct torque control (DTC) . . . 549
3. The major problem in basic DTC scheme . . . 550
   3.1. Variable inverter switching frequency . . . 550
   3.2. High torque ripple . . . 550
   3.3. The need for high-speed processor . . . 550
4. Some DTC improvements to solve problems . . . 552
   4.1. Switching control strategies . . . 552
   4.2. DTC based on space vector modulation . . . 552
      4.2.1. DTC with voltage SVM . . . 552
      4.2.2. DTC with flux SVM . . . 552
   4.3. Constant switching frequency of torque controller . . . 554
   4.4. Predictive control scheme . . . 554
   4.5. Intelligent control techniques . . . 554
5. DTC for EV applications . . . 555
   5.1. Road load and tractive force . . . 555
   5.2. Motor ratings and transmission . . . 555

* Corresponding author at: Universiti Teknologi Malaysia, Department of Energy Conversion, Faculty of Electrical Engineering, 81310 UTM Skudai, Johor, Malaysia. Tel.: +607 553 6139; fax: +607 556 6272.
E-mail addresses: tole@ee.uad.ac.id, thsutikno@ieee.org (T. Sutikno), nikrumzi@fke.utm.my, nikrumzi@ieee.org (N.R.N. Idris), auzani@utem.edu.my, auzani@ieee.org (A. Jidin).

1364-0321/$ - see front matter
http://dx.doi.org/10.1016/j.rser.2014.01.040

6. Reliability of DTC for EV applications . . . 556
7. Conclusion . . . 556
References . . . 557

1. Introduction

The automobile sector is one of the key problem areas in global warming [1]. With demand for automobiles growing rapidly, the supply of oil will diminish, the price of oil will rise sharply and automobile transportation will face a crisis. Without aggressive policy measures, the rapid growth in automobiles on a global scale will increase emissions and result in the further degradation of human health and the environment. To reduce emissions, an alternative technology such as electric vehicles (EV) is one of the options for future transportation. With ever increasing concerns about energy efficiency and environmental protection, the pace of development of EVs for mass marketing has accelerated [2–4].

An EV drive system must include the major features are summarized as follows [5,6]: (i) high instant power and high power density; (ii) high torque at low speeds for starting and climbing, as well as high power at high speed for cruising; (iii) very wide speed range including constant-torque and constant-power regions; (iv) fast torque response; (v) high efficiency over wide speed and torque ranges; (vi) high efficiency for regenerative braking; (vii) high reliability and robustness for various vehicle operating conditions; and (viii) reasonable cost. Therefore, selection of a proper drive and control method are the most important factors in EVs; in addition, robust energy management is the other major crucial element of an EV [7,8].

A comparison of electric motors concluded that the induction motor (IM) is the best selection for EV applications owing to its robustness, low price, mature technology and maintenance-free operation. From the control system theory point of view, the control method is the key for improving motor efficiency, lengthening battery life and as result increasing the driving distance [9–11]. Today, sensorless control as a variable frequency drive is the mature technology among various motor drives. The sensorless control is suitable for critical applications such EV and has advantages in terms of reliability, efficiency improving and energy savings [12]. The two most popular sensorless control methods of IM are field oriented control (FOC) and direct torque control (DTC). Unlike FOC, DTC does not require coordinate transformation, pulse width modulator (PWM) signal generators, current controllers and a position encoder, which introduces delays and requires a mechanical transducer. In spite of its simplicity, DTC provides fast instantaneous torque control in the steady state and under transient operating conditions with simple control structure [13,14]. Since an EV drive system must feature a fast torque response, reasonable cost, reliability and robustness, the DTC of IM appears to be very convenient for EV applications [15–17].

This paper briefly reviews the direct torque control of induction motors as well as its implementation for EV applications. Section 1 introduces that selection of the proper electric drive should be addressed in the development of EVs for future green transportation. Section 2 discusses the basic DTC technique based on hysteresis controllers. Section 3 is devoted to the overview of the major problems in the basic DTC scheme. Section 4 studies some improvements to the basic DTC. Section 5 will present a critical review of the DTC for EV applications. Section 6 will review the reliability of DTC for EV applications that it can operate for a wide range of speed, and Section 7 is the conclusion. The paper aims to provide important guidelines and insights for future research and development on the DTC of IM drives for sustainable reliability and energy efficient EV applications.

2. Direct torque control (DTC)

DTC offers a much simpler structure than the FOC system. The problem of decoupling the stator current in a dynamic fashion in the FOC is avoided in DTC. This method was proposed by Takahashi [18] and Depenbrock [19] for induction motor drives in the mid-1980s. The basic principle of DTC is to directly select stator voltage vectors (switching states) according to the differences between the reference

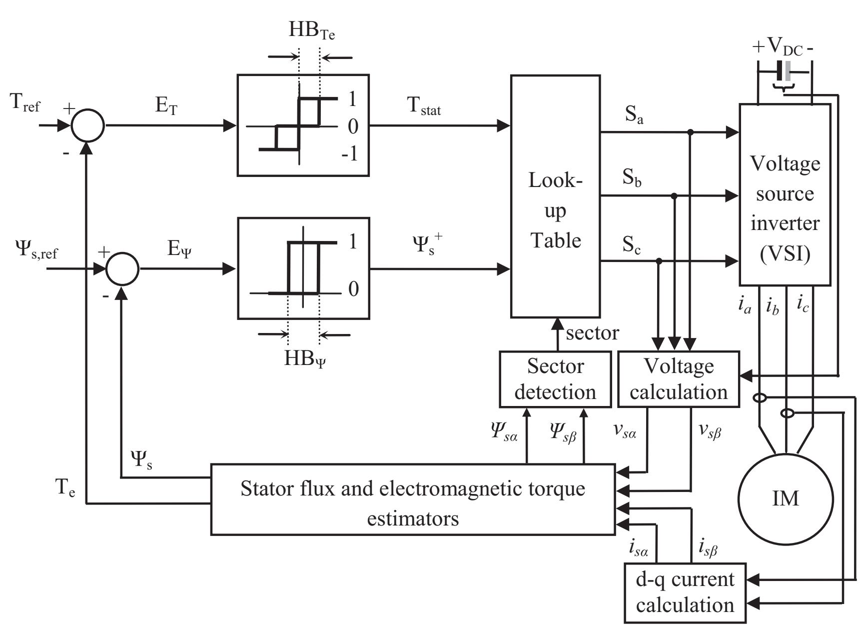

Fig. 1. Control structure of DTC based induction machine.

and the actual values of torque and stator flux linkage. The DTC can provide a very quick and precise torque response without the need for a complex field orientation block and inner current regulation loop. Hence, DTC is very well suited for operation at saturated voltage. Fig. 1 shows a simple structure of hysteresis-based DTC based on the work of Takahashi [18]. A decoupled control of torque and flux was established to permit fast instantaneous control. The stator flux is controlled using a 2-level hysteresis comparator, while the electromagnetic torque is controlled using a 3-level hysteresis comparator. The outputs of the comparators, along with sector flux information, are used to index the look-up table, to select the appropriate voltage vectors to control simultaneously both the stator flux and the torque. The most significant element that can guarantee a satisfactory DTC performance is the estimation of the stator flux and the torque [14,18–21].

In order to estimate the stator flux and the electromagnetic torque, several parameters need to be determined. The mathematical model to be used is tailored to the needs of controlled drives. With considering "Stator flux and electromagnetic torque estimators" block in Fig. 1; first, the stator currents from the motor I_a and I_b are transformed into α–β coordinates, which are adequately suited to the DTC algorithm, as follows [7,14,18–20,22,23]

$$I_\alpha = I_a \tag{1}$$

$$I_\beta = \frac{\sqrt{3}}{3}(I_a + 2I_b) \tag{2}$$

At the same time, by using the switching status (S_a, S_b and S_c) produced by the switching table, the stator voltages in the α–β reference frame are determined:

$$V_\alpha = \frac{V_{dc}}{3}(2S_a - S_b - S_c) \tag{3}$$

$$V_\beta = \frac{\sqrt{3}}{3}V_{dc}(S_b - S_c) \tag{4}$$

Then, using the calculated I_α, I_β, V_α and V_β, the estimation of the stator flux in α–β coordinates is performed as follows:

$$\varphi_\alpha = \varphi_{\alpha_{old}} + (V_\alpha - R_S I_\alpha)T_s \tag{5}$$

$$\varphi_\beta = \varphi_{\beta_{old}} + (V_\beta - R_S I_\beta)T_s \tag{6}$$

Finally, Eq. (7) calculates the flux magnitude by using a square root calculation, whereas the electromagnetic torque is estimated through Eq. (8).

$$\varphi_s = \sqrt{\varphi_\alpha^2 + \varphi_\beta^2} \tag{7}$$

$$T_e = \frac{3}{4}P(I_\beta \varphi_\alpha - I_\alpha \varphi_\beta) \tag{8}$$

The original scheme is based on hysteresis controllers, where the output status from the controllers, together with the sector flux information, are used to select the optimized voltage vectors from the look-up table to satisfy simultaneously both flux and torque references. The flux vector is controlled to form a circular flux shape [18].

3. The major problem in basic DTC scheme

In spite of its simplicity, the basic DTC scheme based on hysteresis controllers causes some quite major drawbacks such as variable inverter switching frequency, high torque ripple and hence high sampling requirement to minimize the problems for digital implementation [14,20,21,23–28].

3.1. Variable inverter switching frequency

In the basic DTC, the switching frequency of voltage source inverter (VSI) is totally contributed by the switching in the hysteresis comparators [18]. The slopes of torque and flux, which relatively affect the switching in their hysteresis comparators, vary with operating conditions (i.e. rotor speed, stator and rotor fluxes and DC link voltage) [28–31]. This causes the switching frequency of VSI also to vary with operating conditions. For this reason, the switching devices cannot be fully utilized to maximum frequency capability for most operating conditions, since the selection of hysteresis bandwidth is based on the worst conditions [29]. Consider the torque slope in a discrete form which is given by Eq. (9).

$$\text{Torque slope} = \frac{T_{e,n+1} - T_{e,n}}{\Delta t} = -T_{e,n}\left(\frac{1}{\sigma\tau_s} + \frac{1}{\sigma\tau_r}\right) + \frac{3}{2}P\frac{L_m}{\sigma L_s L_r}[(v_{s,n} - j\omega_r \Psi_{s,n}) \cdot j\Psi_{r,n}] \tag{9}$$

where T_e: electromagnetic torque; $\boldsymbol{\Psi_s}$: stator flux linkage space vectors in stationary reference frame; $\boldsymbol{\Psi_r}$: rotor flux linkage space vectors in stationary reference frame; ω_r: rotor electrical speed in rad/s; v_s: stator voltage space vector in stationary reference frame.

Eq. (9) indicates that the torque slope depends on the stator flux, rotor flux, the speed and the stator voltage.

3.2. High torque ripple

In digital implementation, the output torque is calculated, and the appropriate switching states are determined at fixed sampling time (which is DT in Fig. 1). This, however, causes a delay between the instant the variables are sampled (i.e. the instant torque is calculated) and the instant the corresponding switching status passes to the inverter. Because of that, the torque ripple cannot be restricted exactly within the hysteresis band. If the band is set too small, this, however, does not minimize the torque ripple. This is because incidents of overshoot in the estimated torque above the torque hysteresis band may occur and hence cause the reverse voltage vector to be selected. The selection of the reverse voltage vector as mentioned previously causes the torque to decrease rapidly and as a result the torque ripple increases [29,32–35].

3.3. The need for high-speed processor

Reducing torque ripple by lowering the band width of the hysteresis comparator would be fruitless when the processor used has a limited sampling frequency. All the constraints which have been mentioned above can be eliminated if a high-speed processor is utilized, where the discrete hysteresis controller performs similarly to the analogue based comparator. The rapid decrease of torque due to the selection of reverse voltage can be avoided if the sampling time (DT) is sufficiently decreased [33,34].

In our previous researches [21,23,33,36], some experimental results of output torque ripple obtained in hysteresis-based DTC at different applied sampling frequencies and/or torque hysteresis bands are presented as shown in Fig. 1(a)–(c). For each case, the control of torque at 6 N m was performed at the same load torque condition so that the rotor speed operated at around 400 rpm. The nominal level of torque hysteresis band is HB_{Te} (0.9 N m) and the minimum sampling time achievable using the digital signal processing (DSP) is 55 µs, i.e. DT = 55 µs.

From Fig. 2(a), the output torque ripple is high when the torque hysteresis band is set to twice HB_{Te}. Thus, to reduce the torque

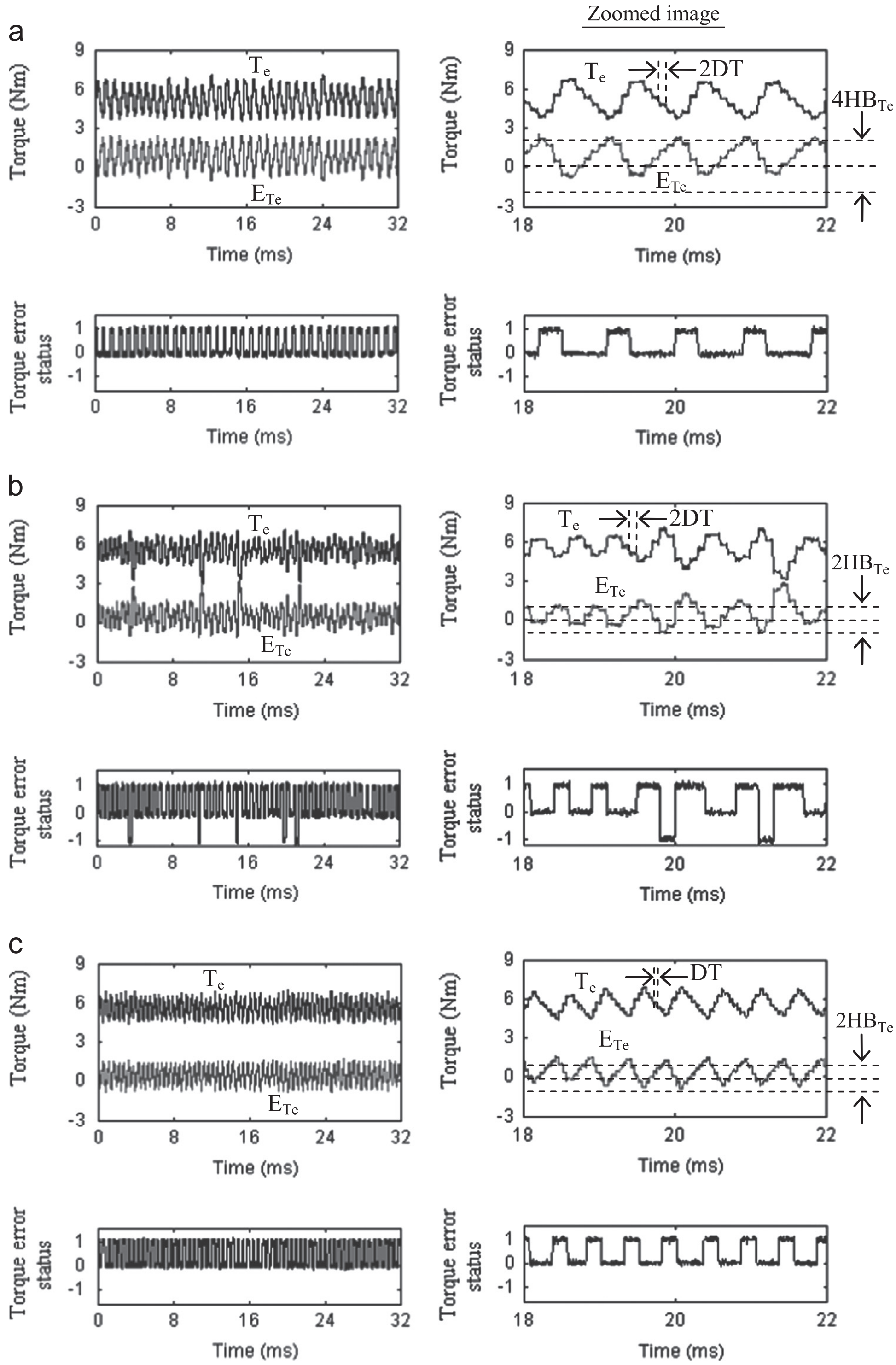

Fig. 2. Experimental results of control of output torque utilizing three-level hysteresis comparator (in hysteresis based-DTC). (a) Hysteresis band = $2HB_{Te}$, sampling time = 2DT, (b) hysteresis band = HB_{Te}, sampling time = 2DT and (c) hysteresis band = HB_{Te}, sampling time = DT [26].

ripple of the basic DTC scheme, one can ideally reduce the hysteresis band. Fig. 2(b) shows the results of output torque control when the torque hysteresis band reduces to HB_{Te}. However, owing to the sampling time used in Fig. 2(a) and (b) being twice the nominal DT (i.e. 110 μs), in practice this leads to incorrect or reverse voltage vector selections (where $T_{stat} = -1$), which causes rapid decreases in output torque and hence increases the torque ripple, as noted in Fig. 2(b). Therefore, to eliminate reverse voltage vector selections, the sampling time needs to be reduced, as demonstrated in Fig. 2(c), whereby the sampling is set to DT. Obviously, as seen in Fig. 2(c), the output torque ripple decreases and no active voltage vector is selected to reduce the torque.

Basically, the output torque ripple can be reduced by reducing the band width of hysteresis comparator to the appropriate value. The selection of the appropriate band width is based on the worst operating conditions. This will ensure the switching frequency of switching devices does not exceed its limit (or thermal restriction). It is also desirable to use a high speed processor to keep the ripple within the band, in such a way that the discrete hysteresis controller will perform like the analogue one. The best way to perform the DTC algorithm at the highest sampling rate with a low cost and fast speed processor is the use of Field Programmable Gate Arrays (FPGA) [23].

4. Some DTC improvements to solve problems

As seen in the above overview, the basic DTC has some disadvantages. Several variations to its original structure (which referred to DTC as hysteresis-based) were proposed to improve the performance of DTC of induction machines. Noticeably, most research projects in recent decades have aimed to overcome the inherent disadvantages of hysteresis-based DTC schemes, such as variable switching frequency and high torque ripple. Some of those improvements will be presented in this section.

4.1. Switching control strategies

The various methods of switching techniques in DTC are summarized in Fig. 3, which shows a typical torque and the corresponding three-phase inverter voltage waveforms, assuming the orientation of the stator flux is in sector 5.

To increase and to reduce the flux, while at the same time increasing the torque in this sector, the preferable voltage vectors are [0 0 1] and [1 0 1], respectively. The zero voltage vectors (either [0 0 0] or [1 1 1]) are used to reduce torque. The torque waveforms for a hysteresis-based controller with the width of the hysteresis marked as δT are shown in Fig. 3(a). The torque overshoots and undershoots beyond and below the hysteresis bands will occur owing to the delay in the microprocessor implementation or sensors. The positive slope is high at low speed, which will increase the possibility of the torque touching the upper band, thus selecting the reverse voltage to reduce the torque. The method, which employs fixed switching but with the whole sampling period applied with a single voltage vector, is depicted in Fig. 3(b) and (c) shows the controlled duty cycle method in which various methods can be used to determine the duty cycle δ for every sampling period Ts. Fig. 3(d) depicts the method which synthesizes the voltage using SVM technique [28,30,35,38]. The fixed switching frequency methods require a fast processor for realization since the duty cycles or voltage vectors need to be calculated for every sampling period, particularly when a small sampling period is required for appreciably small torque ripple [29,36,37].

4.2. DTC based on space vector modulation

The most popular variation of DTC of induction motor drives is the one that is based on space vector modulation (SVM), which is normally referred to as DTC–SVM [22,25,39–44]. The advantages provided by this scheme not only solve the inherent problems in hysteresis-based DTC. The major difference between hysteresis-based DTC and DTC–SVM is the way the stator voltage is generated. In hysteresis-based DTC the applied stator voltage depends on voltage vectors, which are selected from a look-up table. The selections are based on the requirement of the torque and flux demand obtained from the hysteresis comparators. On the other hand, in DTC–SVM, a stator voltage reference is calculated or generated within a sampling period, which is then synthesized using the space vector modulator. The stator voltage reference vector is calculated based on the requirement of torque and flux demands.

4.2.1. DTC with voltage SVM

Fig. 4 presented a block diagram of DTC with voltage SVM (DTC–SVM with closed-loop torque and stator flux) [24,44]. The outputs of the PID controllers are $V_{\Psi c}$ and V_{Tc} representing the reference stator voltage components of the PI stator flux and torque controllers, respectively. Then, the DC voltage commands are transformed into stationary reference frames ($\alpha\beta$), and as outputs are $V_{s\alpha c}$ and $V_{s\beta c}$. These outputs are forwarded to the SVM block. The DTC with voltage SVM can be seen as hysteresis DTC in which the switching table is replaced by a SVM, and a hysteresis torque and stator flux controllers are replaced by PI controllers. As a result, the torque and flux are directly controlled in closed loops, and therefore the DTC–SVM will operate at a constant switching frequency to reduce torque and flux ripples.

4.2.2. DTC with flux SVM

Further simplification of the hysteresis DTC can be achieved by flux vector modulation, as shown in Fig. 5. A PI controller is used

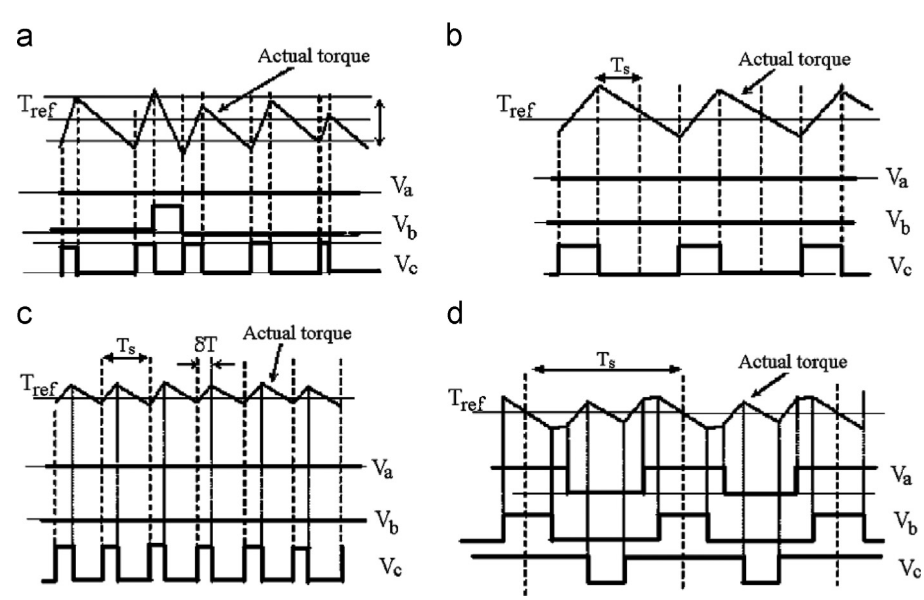

Fig. 3. Typical torque waveforms in various switching strategies of DTC. (a) Hysteresis-based controller. (b) Fixed switching torque. (c) Fixed switching torque with controlled duty ratio. (d) Fixed switching torque with space-vector modulation [30].

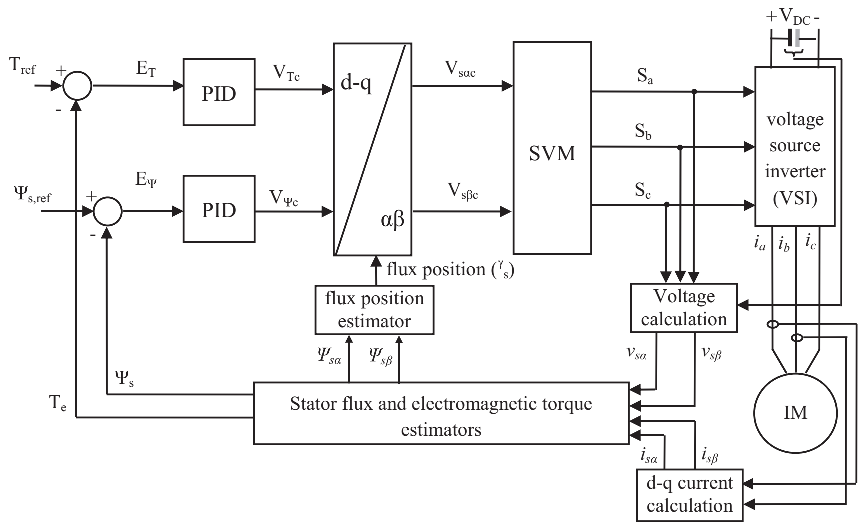

Fig. 4. DTC with voltage SVM.

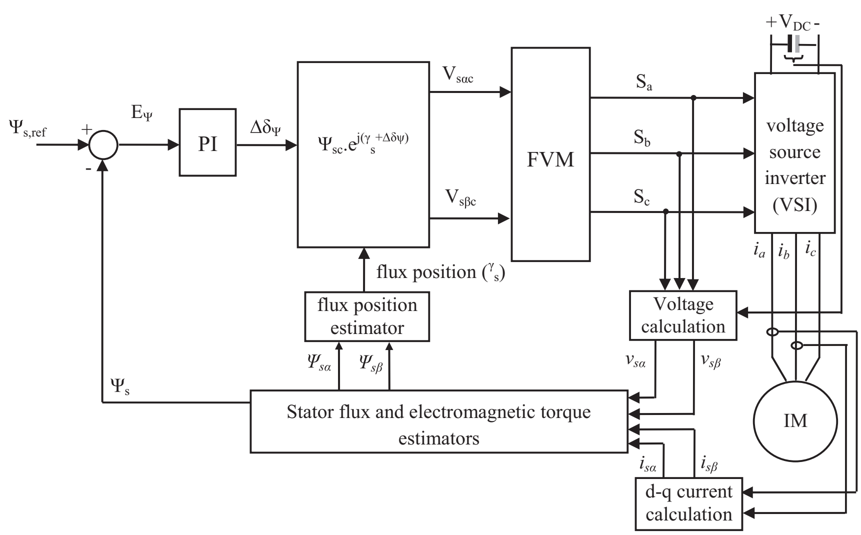

Fig. 5. DTC with voltage FVM.

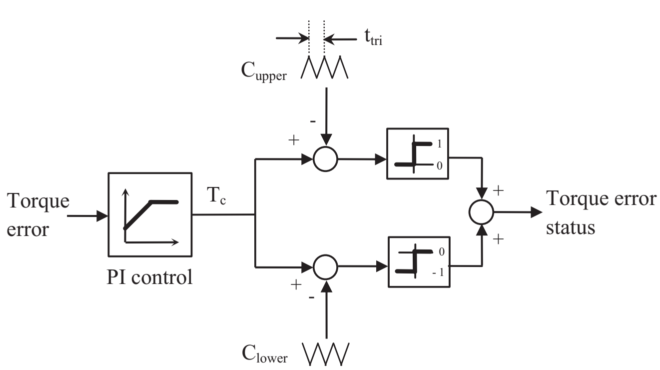

Fig. 6. Constant frequency torque controller (CFTC) [30].

for torque adjustment, and its output generates an increment in the torque angle ($\Delta_{\delta\Psi}$). If the rotor and flux magnitude are assumed equal, so the changing of the torque angle (δ_{Ψ}) can be used to control the torque which corresponds to the increment of the stator flux vector ($\Delta_{\Psi s}$). The estimated flux position and changing of the torque angle are used to calculate the commanded stator flux vector. Then, the outputs of the commanded stator flux vector are directly used to calculate the VSI switching states [25,44].

Owing to the regular sampling in SVM, the DTC–SVM produces constant switching frequency as opposed to the variable switching frequency in hysteresis-based DTC, albeit at the expense of more complex implementation [44]. The generation of reference voltage often involves complex calculation. For example: Habetler [42] used dead-beat control with several complicated equations (i.e. quadratic equations) to generate the reference voltage in real-time and [25] utilized predictive control of stator flux error vector to estimate the reference voltage and needed extra calculation on the synchronous angular velocity. Others include the use of proportional–integral current controller [41], stator flux vector error [39,45,46], proportional–integral torque and flux controllers [22,47,48] and predictive and dead-beat controllers [43,49]. Moreover, the implementation of DTC–SVM becomes complicated as the reference voltage needs to modify whenever it passes outside the hexagon, particularly during a large torque demand. Ultimately, all of the proposed methods complicate the basic control structure of DTC drive systems as originally proposed.

4.3. Constant switching frequency of torque controller

In order to provide a constant switching frequency the torque hysteresis controller can be replaced with the technique that superimposes the torque error with a dithering signal [50] or comparing the error with a triangular waveform [37,51]. In so doing the simple structure of original DTC can be retained as compared to that of using SVM technique. Using the dithering signal it can effectively minimize the torque ripple even performing DTC at limited sampling frequency. On the other hands, applying a triangular carrier-based in controlling the torque requires a proper PI controller as shown in Fig. 6 [37]. This technique has gained further improvement in minimizing the torque ripple significantly by enlarging the carrier frequency even for application of processor with limited sampling frequency, as reported in [51]. Fig. 7 depicts the experimental results of torque ripple obtained in hysteresis based DTC, DTC with triangular carrier-based [37] and DTC with enlarging carrier frequency [51] for a step change of reference torque.

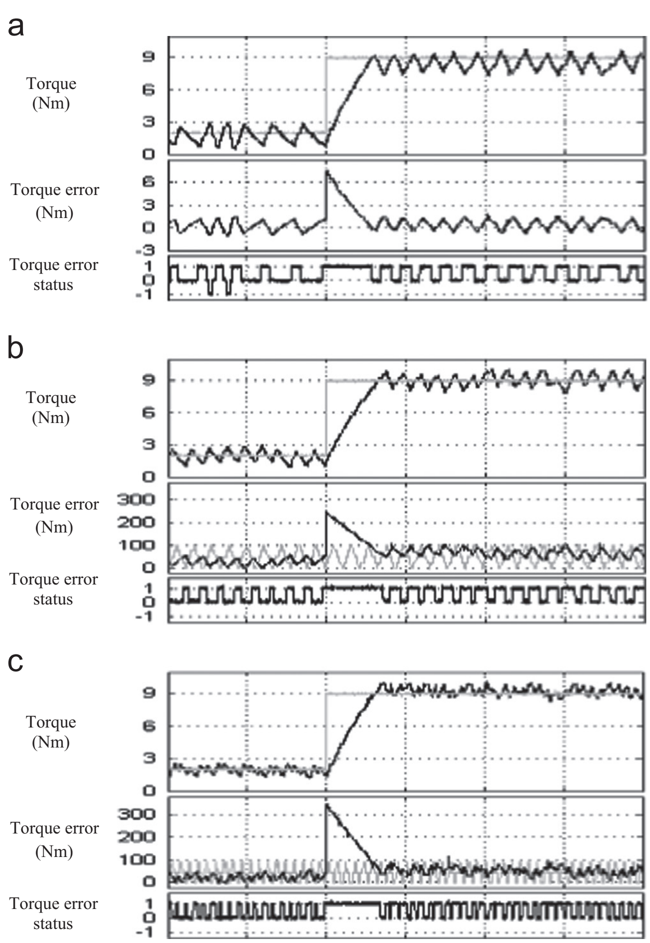

Fig. 7. Experimental results for step response of torque in (a) DTC-hysteresis based, (b) DTC with CFTC [30] and (c) DTC with improved CFTC [44] (time scale: 2 ms/div.).

4.4. Predictive control scheme

Recently, predictive control strategy for DTC has gained a considerable amount of attention, particularly owing to its ability to reduce the torque ripple and switching frequency. In particular, model predictive control (MPC) uses the hysteresis comparators but with the switching table replaced with an online optimization algorithm. The predictive model with input angular shaft speed (Ω_m), stator flux and torque is used to predict the future behaviour of the controlled variables [26,52–54]. The simplified block diagram of the DTC–MPC is shown in Fig. 8.

The important advantages of the MPC are that it is intuitive and simple to understand; straightforward inclusion of non-linearities in the model; simple treatment of constraints; easy to realize; and open to comprise adjustments and expansions depending on specific applications. However, the advantages are offset by troubles when implementing the DTC–MPC, i.e.: larger amount of online calculations compared with hysteresis DTC, and the accuracy of the predictive model has a direct influence on the quality of the predictive controller [44].

4.5. Intelligent control techniques

Intelligent approaches used to enhance the performance of the DTC drive include the use of artificial intelligence (AI), such as neural network, fuzzy logic, genetic algorithm or particle swarm optimization [55–60]. Fuzzy logic controllers can be used in place of the hysteresis comparators and voltage vector selector. Fuzzy logic can also be applied to determine appropriate instances for applying a zero voltage vector within a switching period. Instead

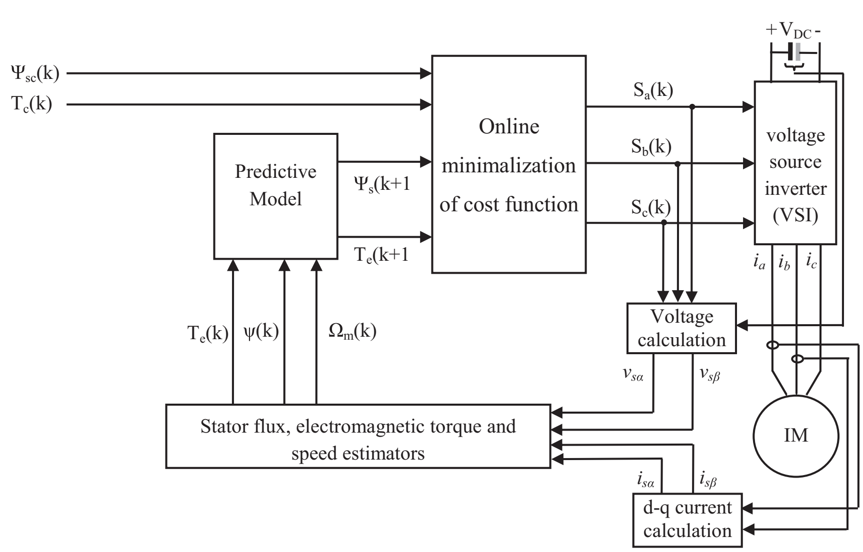

Fig. 8. The simplified block diagram of the DTC–MPC.

of fuzzy logic, a neural network can be used for selecting the voltage vector. But increases in the complexity of the drive to an extent diminish the simple control structure inherent in DTC.

All the techniques discussed above need a high-speed processor for implementation since the duty cycles or voltage vectors need to be calculated for every sampling period, mainly when a small sampling period is needed for considerably small torque and flux ripples. This is usually accomplished using a high-speed digital signal processor (DSP) or field programmable gate array (FPGA).

5. DTC for EV applications

Many control strategies have been proposed for induction motors [7–9]. Among these strategies and as the requirements mentioned in Section 1, DTC appears to be very convenient for EV applications. The required measurements for this strategy are only the input currents, whereas flux, torque and speed can be estimated. The reference speed is used as the control command (input) of the motor controller, which is directly applied by the pedal of the vehicle. Rated flux is used as a reference for below the rated speed (constant torque region), and a flux weakening method can be used for above the rated speed which may imply the need to exceed the supply voltage limits to maintain speed. The current limit and the voltage limit, smooth and precise transition can be obtained, as the onset of the field weakening operation is automatically adjusted in accord with the flux level [21,61].

Fig. 9 gives the configuration of a DTC scheme, and shows how the EV dynamics will be taken into consideration.

5.1. Road load and tractive force

We can evaluate both the driving power and required energy to ensure vehicle operation, taking into consideration the principles of vehicle mechanics and aerodynamics [8,62,63].

The first step is to derive an equation for the tractive force. This is the required energy to propel the vehicle forward and transmitted to the ground/floor through the wheels, if the vehicle has mass m and is moving at a speed v, up an angle α slope, as shown in Fig. 10. The tractive force has to accomplish the following: overcome the rolling resistance (F_{rr}), overcome the aerodynamic drag (F_{ad}), overcome the vehicle weight (mg), and accelerate—this comprises both linear acceleration (F_{la}) and the acceleration force (F_{wa}) of the vehicle [8,62,63]. So, the total tractive force is given as Eq. (10).

$$F_{te} = F_{rr} + F_{ad} + F_{hc} + F_{la} + F_{wa} \tag{10}$$

The rolling resistance F_{rr} is produced by the friction of the vehicle tyre at the roadway contact surface and hardly depends on vehicle speed, tyre pressure and type and road surface characteristic. The rolling resistance is non-linear as Eq. (11).

$$F_{rr} = \mu \text{ mg } \cos(\alpha) \tag{11}$$

where μ: Tire rolling resistance coefficient ($0.015 < \mu < 0.3$).

Aerodynamic drag F_{ad} is the force required to move the friction of the vehicle body through the air. The force is a function of the frontal area, the shape, protrusions such as side mirrors, ducts and air passages, spoilers, etc as Eq. (12).

$$F_{ad} = \frac{1}{2}\rho C_{ad} A_f (v + v_0) \tag{12}$$

where ρ: air density; C_{ad}: aerodynamic drag coefficient ($0.2 < C_{ad} < 0.4$); Af: vehicle frontal area; v: vehicle speed; v_o: head-wind velocity.

The required force to drive the vehicle up a slope is the most simple to calculate. It is only the vehicle weight component that acts along the slope, as Eq. (13). It is also known as climbing resistance (since positive operational sign) or the downgrade force (since negative operational sign).

$$F_{hc} = \pm \text{mg } \sin(\alpha) \tag{13}$$

An additional force is needed when the speed of the vehicle is varying. This force will provide the linear acceleration of the vehicle.

$$F_{la} = ma \tag{14}$$

where a: vehicle acceleration.

However, we should also consider rotational acceleration in addition to the above linear acceleration for a more precise calculation of the required force to accelerate the vehicle. The needed acceleration force by incorporating the gear system efficiency η_g is as Eq. (15).

$$F_{wa} = J\frac{G^2}{\eta_g r^2} a \tag{15}$$

where J: Total inertia (rotor and load); G: Gear ratio; η_g: Gear system efficiency; r: Tire radius.

The F_{la} and F_{wa} values will be negative if the vehicle is slowing down and F_{hc} will be negative if it is going downhill.

5.2. Motor ratings and transmission

The choice of the driving motor on electric vehicles primarily should consider the rated power and rated speed. The higher the power grade selected, the more reserve power is produced and the vehicle's driving feature are improved. But at the same time the volume and weight of the motor will rise rapidly, which can lead

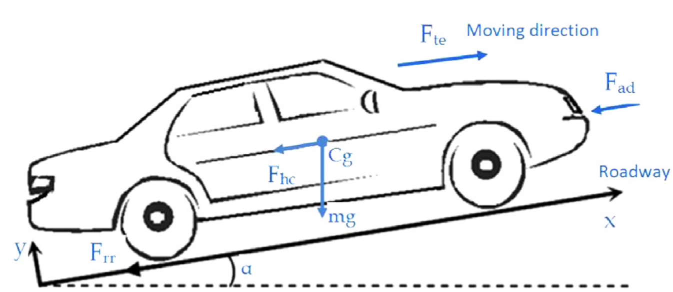

Fig. 10. Elementary forces acting on a vehicle.

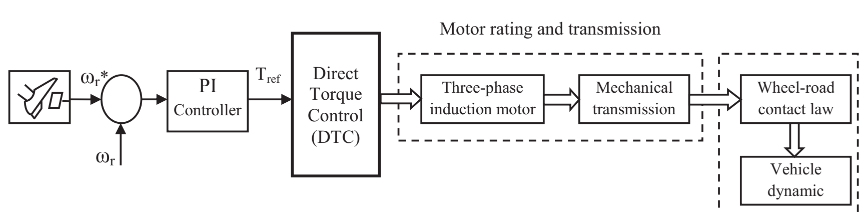

Fig. 9. The configuration of a DTC scheme for EV applications.

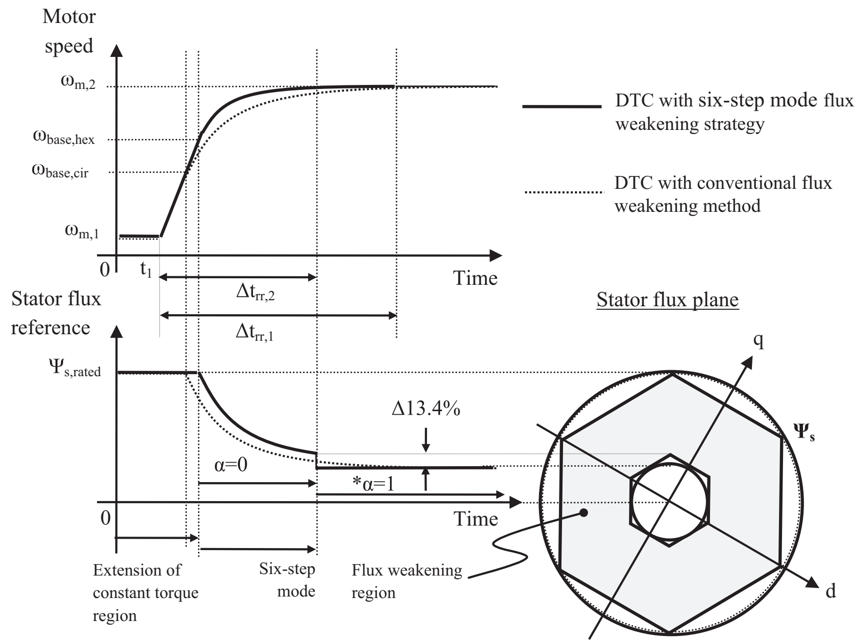

Fig. 11. More rapid motor acceleration achieved with the flux weakening when a step change of reference speed is applied at time t_1.

to a decline in the motor's efficiency. So the motor power should not be too great [8,62,63].

The power necessary to drive a vehicle at a speed v has to compensate for the road load (counteracting forces), i.e.

$$P_{te} = vF_{te} = v\,(F_{rr} + F_{ad} + F_{hc} + F_{la} + F_{wa}) \tag{16}$$

EV has the characters of frequent starting–stopping and acceleration. It is required that the drive system should has accurate control of speed, better tracking performance and high precision of stability. Therefore, drive system has a strong require to the control strategy. DTC is one of the common technologies in drive system. The DTC gets rid of decoupling feedback idea in sector control and changes the direction from rotor to stator. Through controlling the value of stator and the angle of sector can achieve the goal of controlling torque. The DTC has the characters of direct control, simple and efficient structure, good control performance and dynamic speed; but also reduces the power consumption. Considering the above characters, DTC is fit for the control of electric vehicle (EV). However, the above DTC improvements to optimize the efficiency of EV drive according to the driving pattern and operating conditions should be considered to ensure efficiently controlled vehicle, lengthening battery life, safety, stability and reliability at lower cost.

6. Reliability of DTC for EV applications

In recent years DTC as an innovative control method has gained the attraction for EV application, because it can also produces fast torque control of the induction motor and does not need heavy computation on-line, in contrast to FOC. DTC is low cost due to without mechanical speed sensors at the motor shaft. The rotor speed is estimated from sensed stator voltages and currents at the motor terminal. Hence, it can reduces hardware complexity and size of the drive machine, elimination of the sensor cable, improved noise invulnerability, increased reliability, and less maintenance requirements in EV applications [7,64,65].

A wide speed high torque capability is a very important feature in many EV drive applications. In automotive applications, it is usually referred to as a high constant power speed range (CPSR). The availability of wide range of speed operations with the maximum capability of torque is of main concern, especially for the road electric vehicles where multiple gears have to be avoided. DTC is also reliable to provide a robust field weakening as well as supports frequent starting–stopping and acceleration. In practice, a flux weakening strategy is normally used to extend the motor speed operations beyond the base speed and to enhance the capability of torque. The common approach adopted is to estimate the optimal flux level of the motor based on the maximum values of inverter voltage and inverter current [43,66–68].

In order to achieve the fastest torque dynamic response as well as high torque capability in a flux weakening region, the DTC needs to have the capability to operate in six-step mode [69]. In the flux weakening region, a higher capability of torque can be achieved as the overmodulation strategy operates stator voltage in the six-step mode by continuously controlling the flux vector to form hexagonal locus. A conventional flux-weakening method can be used (in order to retain the simple control structure) but with a minor modification. Using the modified method, the magnitude of the hexagonal stator flux is inversely proportional to the rotor speed when the motor operates beyond the base speed [21,33,70]. The control of stator flux magnitude and its corresponding locus for a step change of reference speed from $\omega_{m,1}$ to $\omega_{m,2}$ is illustrated in Fig. 11. However, a step reduction of 13.4% in the flux magnitude is applied as the hexagonal flux locus is instantaneously changed back to the circular locus when the motor speed reaches its target [33,71]. The percentage of the step reduction is actually the maximum difference in magnitude of a hexagonal flux locus. This reduction is to ensure that the output torque can be well-regulated to its reference. Therefore, the modified strategy (with hexagonal flux locus) offers an extended constant torque region and a wider speed range, so $\omega_{base,hex}$ is higher than $\omega_{base,cir}$.

The above presentation has explained that DTC can operate for a wide range of speed, and because it is reliable and capable of providing acceleration, braking and above rated speed (flux weakening) feature of sustainable reliability and energy efficient drives for EV applications.

7. Conclusion

This paper has presented a brief review of DTC of induction motors as well as its implementation for EV applications. The paper has explained that DTC is very suitable for EV applications. DTC is capable of operating over increases and decreases of speed in positive and negative directions (four quadrants) and offers optimal energy management for EV applications. In the first sections, the concepts and major problems of basic DTC are explained and explored. Then some improvements to basic DTC are presented as well as a critical review of DTC for EV applications. The detailed dynamic model of an EV that is associated with DTC drive strategy is explained. It is clear that DTC promises high efficiency in order to extend the running distance per battery charge. The paper is important to provide guidelines and insights for future research and development on DTC of IM drives for sustainable reliability and energy efficiency of EV applications.

References

[1] Abdul-Hak M, Al-Holou N, Mohammad U, Alamir Tamer M, Arafat M. ITS based methodology to reduce energy consumption and emissions. In: Proceedings of the IEEE transportation electrification conference and expo (ITEC); 2012. p. 1–7.
[2] Hirsch RL, Bezdek R, Wendling R. Peaking of world oil production: impacts, mitigation, and risk management. United States Government 2005.
[3] Ahuja D, Tatsutani M. Sustainable energy for developing countries. Trieste, Italy: The Academy of Sciences for the Developing World (TWAS); 2008.
[4] Tie SF, Tan CW. A review of energy sources and energy management system in electric vehicles. Renewable Sustainable Energy Rev 2013;20:82–102.
[5] Chan CC. The state of the art of electric and hybrid vehicles. Proc IEEE. 2002;90:247–75.
[6] Chan CC. The state of the art of electric, hybrid, and fuel cell vehicles. Proc IEEE. 2007;95:704–18.
[7] Faiz J, Sharifian MBB, Keyhani A, Proca AB. Sensorless direct torque control of induction motors used in electric vehicle. IEEE Trans Energy Convers 2003;18:1–10.
[8] Haddoun A, Benbouzid MEH, Diallo D, Abdessemed R, Ghouili J, Srairi KA. Loss-minimization D.T.C. scheme for EV induction motors. IEEE Trans Veh Technol 2007;56:81–8.
[9] Faiz J, Hossieni SH, Ghaneei M, Keyhani A, Proca A. Direct torque control of induction motors for electric propulsion systems. Electr Power Syst Res 1999;51:95–101.
[10] de Santiago J, Bernhoff H, Ekerg, x00E, rd B, Eriksson S, et al. Electrical motor drivelines in commercial all-electric vehicles: a review. IEEE Trans Veh Technol. 2012;61:475–84.
[11] Cheng S, Li C, Chai F, Gong H. Research on induction motor for mini electric vehicles. Energy Procedia 2012;17:249–57 (Part A).
[12] Alsofyani IM. Idris NRN. A review on sensorless techniques for sustainable reliablity and efficient variable frequency drives of induction motors. Renewable Sustainable Energy Rev 2013;24:111–21.
[13] Hoang L-H. Comparison of field-oriented control and direct torque control for induction motor drives. In: IEEE 34th IAS annual meeting conference record of the industry applications conference, vol. 2; 1999. p. 1245–52.
[14] Casadei D, Profumo F, Serra G, Tani A. FOC and DTC: two viable schemes for induction motors torque control. IEEE Trans Power Electron 2002;17:779–87.
[15] Singh B, Jain P, Mittal AP, Gupta JRP. Direct torque control: a practical approach to electric vehicle. In: IEEE Power India conference; 2006. p. 4.
[16] Farasat M, Karaman E. Speed sensorless electric vehicle propulsion system using hybrid FOC–DTC induction motor drive. In: International conference on electrical machines and systems (ICEMS); 2011. p. 1–5.
[17] Rehman H, Longya X. Alternative energy vehicles drive system: control, flux and torque estimation, and efficiency optimization. IEEE Trans Veh Technol 2011;60:3625–34.
[18] Takahashi I, Noguchi TA. New quick-response and high-efficiency control strategy of an induction motor. IEEE Trans Ind Appl 1986;IA-22(5):820–7.
[19] Depenbrock M. Direct self control (DSC) of inverter-fed induction machine. IEEE Trans Power Electron 1988;3(4):420–9.
[20] Idris NRN, Ling TC, Elbuluk MEA. New torque and flux controller for direct torque control of induction machines. IEEE Trans Ind Appl 2006;42:1358–66.
[21] Jidin AB, Idris NRN, Yatim AHM, Elbuluk ME, Sutikno TA. Wide-speed high torque capability utilizing overmodulation strategy in DTC of induction machines with constant switching frequency controller. IEEE Trans Power Electron 2012;27:2566–75.
[22] Lascu C, Boldea I, Blaabjerg F. A modified direct torque control for induction motor sensorless drive. IEEE Trans Ind Appl 2000;36:122–30.
[23] Sutikno T, Nik Idris NR, Jidin A, Cirstea MN. An improved FPGA implementation of direct torque control for induction machines. IEEE Trans Ind Inf 2012:1.
[24] Buja GS, Kazmierkowski MP. Direct torque control of PWM inverter-fed AC motors—a survey. IEEE Trans Ind Electron 2004;51:744–57.
[25] Tripathi A, Khambadkone AM, Panda SK. Stator flux based space-vector modulation and closed loop control of the stator flux vector in overmodulation into six-step mode. IEEE Trans Power Electron 2004;19:775–82.
[26] Beerten J, Verveckken J, Driesen J. Predictive direct torque control for flux and torque ripple reduction. IEEE Trans Ind Electron 2010;57:404–12.
[27] Zhifeng Z, Renyuan T, Baodong B, Dexin X. Novel direct torque control based on space vector modulation with adaptive stator flux observer for induction motors. IEEE Trans Magn 2010;46:3133–6.
[28] Li Y, Shao J, Si B. Direct torque control of induction motor for low speed drives considering discrete effects of control and dead-time of inverter. In: IEEE 32nd IAS annual meeting, IAS '97, conference record of the industry applications conference, vol. 1; 1997. p. 781–8.
[29] Idris NRN. Improved direct torque control of induction motor. Johor Bahru: Universiti Teknologi Malaysia; 2000.
[30] Jun-Koo K, Seung-Ki S. Torque ripple minimization strategy for direct torque control of production motor. In: IEEE 33rd IAS annual meeting of the industry applications conference, vol. 1; 1998. p. 438–43.
[31] Casadei D, Serra G, Tani A. Analytical investigation of torque and flux ripple in DTC schemes for induction motors. In: 23rd International conference on industrial electronics, control and instrumentation (IECON 97), vol. 2; 1997. p. 552–6.
[32] Casadei D, Grandi G, Serra G, Tani A. Switching strategies in direct torque control of induction machines. ICEM 94. France 1994:204–9.
[33] Jidin A. Improved dynamic performance of direct torque control of induction machines. Johor Bahru: Universiti Teknologi Malaysia; 2010.
[34] Noguchi T, Yamamoto M, Kondo S, Takahashi I. High frequency switching operation of PWM inverter for direct torque control of induction motor. In: IEEE 32nd IAS annual meeting, IAS '97, conference record of the industry applications conference, vol. 1; 1997. p. 775–80.
[35] Chuen Ling T, Idris NRN, Yatim AHM. Torque ripple reduction in direct torque control of induction motor drives. In: Proceedings of the national power engineering conference; 2003. p. 88–94.
[36] Jidin A, Idris NRN, Yatim AHM, Sutikno T, Elbuluk ME. An optimized switching strategy for quick dynamic torque control in DTC-hysteresis-based induction machines. IEEE Trans Ind Electron 2011;58:3391–400.
[37] Idris NRN, Yatim AHM. Direct torque control of induction machines with constant switching frequency and reduced torque ripple. IEEE Trans Ind Electron 2004;51:758–67.
[38] Mir S, Elbuluk ME. Precision torque control in inverter-fed induction machines using fuzzy logic. In: 26th Annual IEEE power electronics specialists conference, PESC '95 record, vol. 1; 1995. p. 396–401.
[39] Casadei D, Serra G, Tani K. Implementation of a direct control algorithm for induction motors based on discrete space vector modulation. IEEE Trans Power Electron 2000;15:769–77.
[40] Bolognani S, Zigliotto M. Novel digital continuous control of SVM inverters in the overmodulation range. IEEE Trans Ind Appl 1997;33:525–30.
[41] Khambadkone AM, Holtz J. Compensated synchronous PI current controller in overmodulation range and six-step operation of space-vector-modulation-based vector-controlled drives. IEEE Trans Ind Electron 2002;49:574–80.
[42] Habetler TG, Profumo F, Pastorelli M, Tolbert LM. Direct torque control of induction machines using space vector modulation. IEEE Trans Ind Appl 1992;28:1045–53.
[43] Tripathi A, Khambadkone AM, Panda SK. Dynamic control of torque in overmodulation and in the field weakening region. IEEE Trans Power Electron 2006;21:1091–8.
[44] Kazmierkowski MP, Franquelo LG, Rodriguez J, Perez MA, Leon JI. High-performance motor drives. IEEE Ind Electron Mag 2011;5:6–26.
[45] M Fu, Xu LA.. Sensorless direct torque control technique for permanent magnet synchronous motors. In: Conference record, IEEE industry applications society annual meeting; 1999.1: p. 159–64.
[46] Casadei D, Serra G, Tani A, Zarri L, Profumo F. Performance analysis of a speed-sensorless induction motor drive based on a constant-switching-frequency DTC scheme. IEEE Trans Ind Appl 2003;39:476–84.
[47] Y Xue, X Xu, Habetler TG, Divan DM. A low cost stator flux oriented source variable speed drive. In: Conference record 1990 IEEE industry applications society annual meeting; 1990.1: p. 410–5.
[48] Hoffman F, Janecke M. Fast torque control of an IGBT-inverter fed three-phase a.c drive in the whole speed range—experimental results. In: Sixth European power electronic conference, (Sevilla, Spain); 1995. p. 399–404.
[49] Griva G, Habetler TG, Profumo F, Pastorelli M. Performance evaluation of a direct torque controlled drive in the continuous PWM-square wave transition region. IEEE Trans Power Electron 1995;10:464–71.
[50] Noguchi T, Yamamoto M, Kondo S, Takahashi I. Enlarging switching frequency in direct torque-controlled inverter by means of dithering. IEEE Trans Ind Appl 1999;35:1358–66.
[51] Jidin A, Idris NRN, Yatim AHM, Sutikno T, Elbuluk ME. Extending switching frequency for torque ripple reduction utilizing a constant frequency torque controller in dtc of induction motors. J Power Electron 2011;11:148–55.
[52] Geyer T, Papafotiou G, Morari M. Model predictive direct torque control—Part I: Concept, algorithm, and analysis. IEEE Trans Ind Electron 2009;56:1894–905.
[53] Papafotiou G, Kley J, Papadopoulos KG, Bohren P, Morari M. Model predictive direct torque control—Part II: Implementation and experimental evaluation. IEEE Trans Ind Electron 2009;56:1906–15.
[54] Zeinaly Y, Geyer T, Egardt B. Trajectory extension methods for model predictive direct torque control. In: 26th annual IEEE applied power electronics conference and exposition (APEC); 2011. p. 1667–74.
[55] Orille AL, Sowilam GMA. Application of neural networks for direct torque control. Comput Ind Eng 1999;37:391–4.
[56] Chaikhy H, Khafallah M, Saad A, Chikh K, Es-Saadi M. Comparison between classical and intelligent DTC strategies for induction machine. In: International conference on multimedia computing and systems (ICMCS); 2012. p. 1163–7.

[57] Jadhav SV, Kirankumar J, Chaudhari BN. ANN based intelligent control of induction motor drive with space vector modulated DTC. In: IEEE International conference on power electronics, drives and energy systems (PEDES); 2012. p. 1–6.
[58] Jadhav SV, Srikanth J, Chaudhari BN. Intelligent controllers applied to SVM-DTC based induction motor drives: a comparative study. In: Joint international conference on power electronics, drives and energy systems (PEDES) & 2010 Power India; 2010. p. 1–8.
[59] Yu-hou W, Zhen-ning P, Ti-xiu Z. Research on development of direct torque control. In: International conference on electric information and control engineering (ICEICE); 2011. p. 662–5.
[60] Gadoue SM, Giaouris D, Finch JW. Artificial intelligence-based speed control of DTC induction motor drives—a comparative study. Electr Power Syst Res 2009;79:210–9.
[61] Fuchs EF, Myat MH. Speed and torque range increases of electric drives through compensation of flux weakening. In: International symposium on power electronics electrical drives automation and motion (SPEEDAM); 2010. p. 1569–74.
[62] Haddoun A, Benbouzid MEH, Diallo D, Abdessemed R, Ghouili J, Srairi K. Sliding mode control of EV electric differential system. Greece: ICEM. Chania; 2006.
[63] Khoucha F, Marouani K, Haddoun A, Kheloui A, Benbouzid MEH.An Improved Sensorless DTC Scheme for EV Induction Motors. In: IEEE International electric machines & drives conference, IEMDC '07; 2007. p. 1159–64.
[64] Jezernik K. Speed sensorless torque control of induction motor for EV's. In: Seventh international workshop on advanced motion control; 2002. p. 236–41.
[65] Singh B, Jain P, Mittal AP, Gupta JRP.. Speed sensorless electric vehicle propulsion system using DTC IM drive. In: India international conference on power electronics, 2006 IICPE; 2006. p. 7–11.
[66] Myoung-Ho S, Dong-Seok H, Soon-Bong C. Maximum torque control of stator-flux-oriented induction machine drive in the field-weakening region. IEEE Trans Ind Appl 2002;38:117–22.
[67] Mengoni M, Zarri L, Tani A, Serra G, Casadei D. Stator flux vector control of induction motor drive in the field weakening region. IEEE Trans Power Electron 2008;23:941–9.
[68] Casadei D, Serra G, Stefani A, Tani A, Zarri L. DTC drives for wide speed range applications using a robust flux-weakening algorithm. IEEE Trans Ind Electron 2007;54:2451–61.
[69] Xingyi X, Novotny DW. Selection of the flux reference for induction machine drives in the field weakening region. IEEE Trans Ind Appl 1992;28:1353–8.
[70] Jidin A, Idris N, Yatim AHM, Elbuluk MA. Novel overmodulation and field weakening strategy for direct torque control of induction machines. In: IEEE Industry applications society annual meeting, IAS '08; 2008. p. 1–8.
[71] Jidin A, Idris NRN, Yatim AHM, Sutikno T, Elbuluk MEA. Hybrid DTC–DSC drive for high performance induction motor control. J Power Electron 2011;11:704–12.